JACS
JOURNAL OF THE AMERICAN CHEMICAL SOCIETY
Article
pubs.acs.org/JACS

Chemical Rescue of the Distal Histidine Mutants of Tryptophan 2,3-Dioxygenase

Jiafeng Geng, Kednerlin Dornevil, and Aimin Liu*

Department of Chemistry & Center for Diagnostics and Therapeutics, Georgia State University, 161 Jesse Hill Jr. Drive, Atlanta, Georgia 30303, United States

Supporting Information

ABSTRACT: Tryptophan 2,3-dioxygenase (TDO) is a heme-dependent enzyme that catalyzes the oxidative degradation of L-tryptophan (L-Trp) to *N*-formylkynurenine (NFK). A highly conserved histidine residue in the distal heme pocket has attracted great attention in the mechanistic studies of TDO. However, a consensus has not been reached regarding whether and how this distal histidine plays a catalytic role after substrate binding. In this study, three mutant proteins, H72S, H72N, and Q73F were generated to investigate the function of the distal histidine residue in *Cupriavidus metallidurans* TDO (cmTDO). Spectroscopic characterizations, enzymatic kinetic analysis, and chemical rescue assays were employed to study the biochemical properties of the wild-type enzyme and the mutant proteins. Rapid kinetic methods were utilized to explore the molecular basis for the observed stimulation of catalytic activity by 2-methylimidazole in the His72 variants. The results indicate that the distal histidine plays multiple roles in cmTDO. First, His72 contributes to but is not essential for substrate binding. In addition, it shields the heme center from nonproductive binding of exogenous small ligand molecules (i.e., imidazole and its analogs) via steric hindrance. Most importantly, His72 participates in the subsequent chemical catalytic steps after substrate binding possibly by providing H-bonding interactions to the heme-bound oxygen.

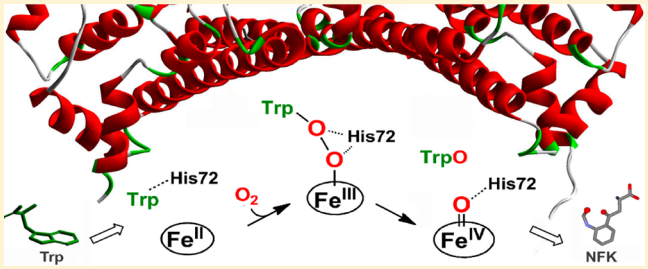

INTRODUCTION

Histidine participates in various important functions in a wide range of proteins and enzymes. Particularly, distal histidines have been shown to play crucial roles in many hemoproteins, and in some cases, they are versatile enough to perform multiple functions. For instance, in hemoglobin the oxy-ferrous complex is stabilized via H-bonding interactions between the distal histidine and O_2. Moreover, the distal histidine in hemoglobin also effectively prevents undesired heme iron oxidation and inhibits interactions between the heme center and competing small molecules such as CO and NO without compromising the binding of O_2.[1] In the present study, we probed the role of a conserved distal histidine in a heme-dependent dioxygenase.

The dioxygenation reaction of tryptophan shown in Scheme 1 is known to be catalyzed by two closely related *b*-type heme-dependent enzymes, tryptophan 2,3-dioxygenase (TDO) and indoleamine 2,3-dioxygenase (IDO). In mammals, TDO is mainly a hepatic enzyme that participates in the initial and rate-limiting step of the kynurenine pathway, which is the primary route of L-Trp metabolism.[2−7] In eukaryotes, the kynurenine pathway is responsible for the major part of the de novo biosynthesis of NAD, an essential redox cofactor in all living systems.[7,8] In addition to mammals, TDO has also been found in other sources such as mosquitoes and bacteria.[6,7,9−13] IDO is an isozyme of TDO and is also involved in the kynurenine pathway. IDO is primarily present in mammals and has a much wider distribution in tissues other than the liver.[10,14] Although both enzymes catalyze the same reaction, TDO is highly substrate specific with L-Trp, whereas IDO exhibits more tolerance toward a collection of indoleamine derivatives.[15−17] TDO is a homotetramer with a total mass of ca. 134 kDa;[18] IDO is monomeric.[19] Although the two enzymes share only ∼10% sequence identity, they exhibit similar active site architectures.[18−20]

It was initially believed that TDO begins its catalytic cycle with deprotonation of the indole NH group of the substrate by an active site base, and the distal histidine is the apparent candidate for playing such a role.[18,21−24] This histidine is a highly conserved residue and replaced by threonine in only three putative TDO sequences.[18] In the crystal structure of the

Scheme 1. Dioxygenation Reaction of L-Trp Catalyzed by IDO and TDO

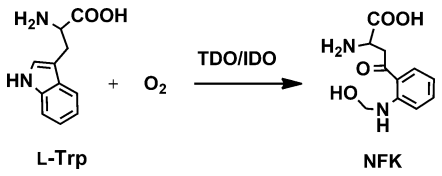

Received: April 30, 2012
Published: June 28, 2012

dx.doi.org/10.1021/ja304164b | J. Am. Chem. Soc. 2012, 134, 12209−12218

binary complex of *Xanthomonas campestris* TDO (xcTDO) and L-Trp, the corresponding distal histidine (His55 in xcTDO amino acid numbering) is H-bonded to the indole group of the substrate, suggesting its involvement in substrate binding.[20] The crystal structures of H55A and H55S variants from xcTDO in binary complexes with L-Trp were reported in a subsequent paper, which show that the aforementioned H-bonding interaction is abolished in the mutant proteins.[25] Since both His55 mutants exhibited detectable activity, the distal histidine was proposed to function as a transition-state stabilizer, rather than an essential base.[25] A detailed model for such a stabilization role still remains to be explored. It has also been shown that the distal histidine is able to prevent formation of the nonproductive ferric enzyme−substrate complex, as revealed by the sharp increase in affinity of L-Trp to the ferric enzyme upon replacement of the distal histidine.[25] On the basis of resonance Raman study of the ternary complex of L-Trp-O_2-TDO from human TDO (hTDO), it was suggested that the distal histidine (His76 in hTDO amino acid numbering) plays a critical role in catalysis by regulating substrate−protein interactions and deprotonating the indole NH group of the substrate to initiate the reaction.[26] Fukumura et al. reported that His76 is involved in regulating the spin state of the heme iron in hTDO and they were also in favor of the acid−base catalyst role of His76.[27] However, 1-methyl-L-Trp (1-Me-L-Trp) was demonstrated to be a slow substrate for human IDO (hIDO), His55 variants of xcTDO, and His76 variants of hTDO, thereby throwing into question the necessity for deprotonation of the indole NH group of the substrate during catalysis.[28] Davydov et al. showed that mutation of His55 in xcTDO or methylation of the indole nitrogen of the substrate had neither observable effect on the spectroscopic properties of the cryoreduced oxy heme moiety nor its annealing behavior, arguing against proton abstraction of the indole group as the initial catalytic step.[29]

Recent computational studies, including density functional theory (DFT), molecular dynamics (MD), quantum mechanics/molecular mechanics (QM/MM) and ONIOM calculations, cast further doubt on the catalytic role of the distal histidine as an active site base by demonstrating that the proton abstraction process is not energetically favorable.[30−33] A recent ONIOM study on xcTDO suggested that the distal histidine, through strengthening H-bonding interactions with the indole moiety, potentially serves as an electrostatic catalyst.[33] It is worth noting that in IDO, a serine residue (S167 in hIDO), which is typically incapable of proton abstraction, occupies the distal histidine position.[19] The S167A mutant in hIDO exhibits similar catalytic activity to that of the wild-type enzyme, indicating that the distal serine residue is not essential for catalysis in IDO.[19,34]

To investigate the function of the distal histidine, especially in the catalytic steps after substrate binding, we performed site-directed mutagenesis, spectroscopic characterizations as well as enzymatic kinetic studies on *Cupriavidus metallidurans* TDO (cmTDO). Our results strengthen the notion that the distal histidine (His72 in cmTDO amino acid numbering) is involved in substrate binding while excluding the possibility that His72 acts as an active site base during catalysis. The chemical rescue assays demonstrate that the catalytic activity of the His72 variants can be restored to a significant degree by an exogenous histidine analogue. Additional stopped-flow UV−vis experiments provide a molecular basis for the observed results from the chemical rescue studies.

MATERIALS AND METHODS

Reagents. L-Trp (99%), 1-Me-L-Trp (95%)*, imidazole (IM) (99%), 2-methylimidazole (2MI) (99%), and 4-methylimidazole (4MI) (≥96%) were purchased from Sigma-Aldrich without further purification. H_2O_2 (30%, v/v) was obtained from Fisher Scientific. The concentration of H_2O_2 was determined based on the extinction coefficient of $\epsilon_{240\ nm}$ = 43.6 M^{-1} cm^{-1}. All the spectroscopic characterizations and enzymatic assays were performed in 50 mM Tris-HCl buffer, pH 7.4, unless otherwise specified.

Mutant Construction, Expression and Purification of cmTDO. The construction of the plasmid encoding His-tagged full-length cmTDO has been reported elsewhere.[18] This plasmid was used as a template for mutant construction in this study. H72S, H72N and Q73F were created using the QuikChange II kit (Stratagene). The oligonucleotide primer sequences used for site-directed mutagenesis were 5′-TTCATCGTCCAGTCCCAGACCACCGAA-3′ for H72S, 5′-TTCATCGTCCAGAACCAGACCACCGAA-3′ for H72N, and 5′-ATCGTCCAGCACTTTACCACCGAACTC-3′ for Q73F. The entire sequences of the three mutants were verified by DNA sequencing. The procedures used for expression and purification of TDO variants were the same as described previously for WT-TDO.[35,36] Briefly, the proteins were purified using a Ni-NTA affinity column on an ÄKTA FPLC system, followed by a Superdex 200 gel-filtration column for salt removal, further purification and buffer exchange. The levels of protein expression and the yields of purified protein for the mutants were similar to WT-TDO. The heme concentrations of the as-isolated ferric proteins were calculated based on their extinction coefficients of Soret band absorption maxima (WT: $\epsilon_{405\ nm}$ = 130 mM^{-1} cm^{-1}; Q73F: $\epsilon_{405\ nm}$ = 120 mM^{-1} cm^{-1}; H72S: $\epsilon_{404\ nm}$ = 120 mM^{-1} cm^{-1}; H72N: $\epsilon_{404\ nm}$ = 120 mM^{-1} cm^{-1}), which were determined using inductively coupled plasma optical emission spectroscopy (ICP-OES) and EPR spin quantitation technique as reported previously.[35,36]

Spectroscopic Characterizations. The optical spectra of cmTDO and its mutants were recorded on an Agilent 8453 UV−vis spectrophotometer at room temperature. The ferrous enzymes were prepared by reducing the ferric proteins with sodium dithionite under anaerobic condition and the corresponding optical spectra were measured with a custom anaerobic cuvette.

X-band EPR spectra were measured in perpendicular mode on a Bruker ER200D spectrometer at 100 kHz modulation frequency coupled with a 4116DM resonator. The measurement temperature was maintained at 10 K using an ESR910 liquid helium cryostat and an ITC503 temperature controller from Oxford Instruments (Concord, MA). The final heme concentration of each EPR sample was 200 μM.

Enzymatic Assays. Steady-state kinetic assays were performed at room temperature using an Agilent 8453 UV−vis spectrophotometer. The enzyme activities of cmTDO and its variants were measured by monitoring formation of the dioxygenation product NFK at 321 nm ($\epsilon_{321\ nm}$ = 3152 M^{-1} cm^{-1}).[18] The reaction rates were calculated from the initial velocities of NFK formation. L-Trp stock solution was prepared freshly in the reaction buffer (i.e., 50 mM Tris-HCl, pH 7.4) in a warm water bath. Reactions were performed in the presence of an excess amount (i.e., 1 mM) of L-ascorbate, as typically used by many others.[18,23,26,37] TDO was added at the end to initiate the reaction. Each reaction was repeated in triplicate to determine the initial velocity. The kinetic parameters were obtained by varying the concentration of the substrate and fitting the reaction rates at different substrate concentrations to the Michaelis−Menten equation:

$$v/[E] = k_{cat}[S]/(K_m + [S]) \quad (1)$$

where v is the steady state velocity; [E] is the concentration of enzyme; [S] is the concentration of substrate; k_{cat} is the catalytic turnover constant; and K_m is the Michaelis−Menten constant. At least two different preps of protein were measured using the same method for each mutant and there was no observable difference in the kinetic parameters between preps.

In the chemical rescue assays, rescuing reagent (IM, 2MI, or 4MI) was added to the reaction system prior to the addition of enzyme. The $K_{activation}$ values of 2MI from the His72 mutants were determined by

varying the concentration of 2MI while L-Trp concentration was kept constant (i.e., 1 mM) and calculating the corresponding rescued dioxygenase activities, which were the differences between the reaction rates determined in the presence and absence of 2MI. The rescued enzymatic reaction rate was plotted as a function of 2MI concentration, and the data were fit to eq 1 with the Michaelis–Menten constants of the fitting results assigned as the $K_{activation}$ values. The kinetic parameters of the His72 mutants under saturating 2MI concentration (i.e., 50 mM) condition were measured by varying the concentration of substrate and analyzing the reaction rates at different substrate concentrations by Michealis-Menten curve fitting.

Rapid Reaction Studies. Transient kinetic measurements were performed at 4 °C using an Applied Photophysics (Leatherhead, UK) SX20 stopped-flow spectrometer equipped with a photodiode array detector. The sample handling unit of the SX20 spectrometer was housed in an anaerobic chamber from COY Laboratory Products (MI, U.S.). All reagents, including enzymes, L-Trp, and imidazoles were prepared in 50 mM Tris-HCl buffer, pH 7.4. The experimental data were analyzed using the ProK software package from Applied Photophysics.

RESULTS

To probe the catalytic role of His72, two variants, H72S and H72N, were constructed. The mutation of His72 to serine mimics the scenario in IDO. The asparagine in H72N is incapable of functioning as an acid–base catalyst but potentially capable of maintaining the H-bonding interaction to Fe-bound oxygen in which His72 participates. A third mutant, Q73F, was also created. Gln73 is a conserved residue adjacent to His72 with the apparent role of maintaining the proper orientation of His72 in the active site. The substitution of Gln73 by a bulky and hydrophobic amino acid such as phenylalanine should not directly modify His72, but would likely change its physical position.

Spectroscopic Characterization of cmTDO. Ferric cmTDO showed an axial EPR signal at g = 6.18, 5.73, and 2.00 (Figure 1A), representing a high-spin ferric heme center with approximate axial symmetry.[36] Similar axial signals with slight rhombicity were observed in H72S and H72N (Figure 1C and 1D), which suggests that the replacement of His72 had little effect on the overall protein conformation and heme symmetry. However, a minor low-spin ferric species with very broad absorption feature at g = 2.98, 2.31, and 1.58 was identified in both His72 variants (Figure 1C,D). This species is assigned as an imidazole-ligated hexa-coordinated heme based on the similarity of its g-factors to those of other histidine-coordinated hemoproteins with imidazole in the sixth coordination position.[38−40] The EPR parameters of this low-spin species also exhibit a very large g_{max} value (2.98) and g-anisotropy value ($|g_x - g_z|$ = 1.40), thereby suggesting the formation of a so-called highly anisotropic low-spin (HALS)-like heme species.[41−44] The coordinating imidazole was most likely introduced into the active site of the His72 mutants during the initial protein purification step via affinity chromatography, in which buffer solutions containing a high concentration of imidazole (i.e., 500 mM) were used during the gradient elution of the target proteins. Even though gel-filtration chromatography was utilized to remove imidazole in the subsequent purification step, a small portion of heme (<10%, calculated based on spin quantitation of the high-spin ferric heme) from the His72 variants remained to be coordinated by imidazole, giving rise to the HALS-like species. Proteins of His72 variants obtained from different preps showed similar percentage of this minor species. Q73F, on the other hand, presented a more axial high-spin signal at g = 5.83 and 2.00 with no additional low-spin signal (Figure 1B). All the EPR parameters for cmTDO are summarized in Table 1.

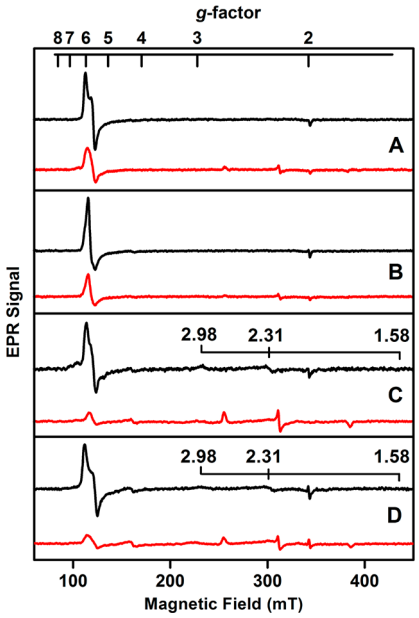

Figure 1. EPR spectra of cmTDO (200 μM heme concentration) in the absence (black) and presence (red) of L-Trp (10 mM). (A) WT-TDO, (B) Q73F, (C) H72S, and (D) H72N. The minor low-spin species in His72 mutants were labeled for clarification. Experimental conditions: temperature, 10 K; microwave frequency, 9.65 GHz; microwave power, 3 mW; and modulation amplitude, 0.5 mT.

Table 1. EPR Parameters of cmTDO

sample	g-values		
	high-spin	low-spin #1	low-spin #2
WT-TDO	6.18, 5.73, 2.00	N/A	N/A
WT-TDO + L-Trp	5.72, 2.00	N/A	2.69, 2.19, 1.80
Q73F	5.83, 2.00	N/A	N/A
Q73F + L-Trp	5.80, 2.00	N/A	2.69, 2.20, 1.80
H72S	6.04, 5.69, 2.00	2.98, 2.31, 1.58	N/A
H72S + L-Trp	5.67, 2.00	N/D[a]	2.70, 2.21, 1.79
H72N	6.16, 5.65, 2.00	2.98, 2.31, 1.58	N/A
H72N + L-Trp	6.03, 2.00	N/D[a]	2.70, 2.21, 1.79

[a]N/D: undetermined.

Upon addition of L-Trp to wild-type cmTDO, there was a substantial decrease in the high-spin ferric signal concomitant with the appearance of a new low-spin ferric species at g = 2.69, 2.19, and 1.80 (Figure 1A). This substrate-driven spin-transition process was characterized in TDOs from different sources using different spectroscopic methods.[26,45−47] A similar phenomenon was observed in IDO as well.[34,48−50] All of the cmTDO mutants showed the same trend of change in spin-transition upon substrate binding (Figure 1B–1D). By comparing its g-values with those of the hydroxide-bound ferric low-spin species identified in other hemoproteins,[45,51] this newly produced low-spin species can be assigned as such. It has been proposed that the hydroxide ligand is derived from an active site water,[26,36,46] which has been shown to be H-bonded to the amine group of the substrate in the ligand-bound crystal structure of xcTDO.[20,25] In His72 variants, the spin-transition process was more pronounced than those observed in WT-

dx.doi.org/10.1021/ja304164b | J. Am. Chem. Soc. 2012, 134, 12209–12218

Table 2. Steady-State Kinetic Properties of TDO

source	protein	k_{cat} (s^{-1})	K_m (mM)	k_{cat}/K_m (mM^{-1} s^{-1})	% of activity (k_{cat}/K_m)	ref
cmTDO[a] (pH 7.4)	WT	12.0 ± 0.4	0.22 ± 0.01	55	100	this work
	Q73F	3.6 ± 0.2	1.1 ± 0.1	3.3	6.0	
	H72S	0.55 ± 0.01	0.42 ± 0.02	1.3	2.4	
	H72S + 2MI[b]	3.1 ± 0.2	0.43 ± 0.06	7.2	13	
	H72N	0.060 ± 0.003	0.62 ± 0.08	0.097	0.17	
	H72N + 2MI[b]	0.23 ± 0.01	0.43 ± 0.04	0.53	0.96	
hTDO (pH 8.0)	WT	6.12 ± 0.02	0.0825 ± 0.0038	74.2	100	27
	H76A	0.04 ± 0.00	0.488 ± 0.051	0.09	0.12	
hTDO (pH 7.0)	WT	2.1	0.19	11.05	100	26, 46
	H76A	0.2	0.5	0.4	3.6	
	H76S	0.03	1.2	0.025	0.23	
xcTDO (pH 7.5)	WT	19.5 ± 1.2	0.114 ± 0.001	171.1	100	25
	H55A	2.86 ± 0.10	0.133 ± 0.007	21.5	13	
	H55S	2.6 ± 0.01	0.197 ± 0.002	13.2	7.7	

[a]The steady-state kinetic assays were performed in 50 mM Tris-HCl buffer, pH 7.4, in the presence of 1 mM L-ascorbate at room temperature. See more details in the "Materials and Methods" section. [b]The kinetic parameters were determined in the presence of 50 mM 2MI.

TDO and Q73F, suggesting that mutation of His72 alters the binding conformation of the substrate and thus affects the pK_a of the active site water. Moreover, the original imidazole-induced HALS-like species significantly decreased in intensity upon substrate binding (Figure 1C,D), indicating that the active site water competes with imidazole to ligate to the heme center in the presence of L-Trp.

Figure S1 of the Supporting Information, SI, shows the optical absorption spectra of ferric and ferrous cmTDO and its mutants in the absence and presence of L-Trp. Q73F shares similar optical spectra with WT-TDO in almost every aspect. Despite some moderate alterations, there are no substantial spectral changes upon replacement of His72. After addition of excess substrate to cmTDO and its mutants, the Soret band decreased in intensity in both ferric and ferrous states and red-shifted approximately 1 nm in the ferric state. The visible bands were not observably sensitive to substrate binding. Table S1 of the SI summarizes the key features of the optical absorption data of cmTDO and its mutants. It should be noted that the spectral features of as-isolated cmTDO change as a function of pH. The mutant proteins follow the same pattern as that observed in the wild-type enzyme (Figure S2 of the SI).

Steady-State Kinetic Study of cmTDO. The steady-state kinetic assays of cmTDO and its derivatives were performed at room temperature. The kinetic parameters are listed in Table 2. For WT-TDO, the k_{cat} and K_m values were determined to be 12.0 ± 0.4 s^{-1} and 0.22 ± 0.01 mM, respectively. Collectively they lead to a k_{cat}/K_m value of 55 mM^{-1} s^{-1}. The mutation of Gln73 to Phe caused the least decrease among the cmTDO mutants in the turnover number to ~30% of the value in WT-TDO. It did, however, introduce the most distinct influence on the K_m value − a ca. 5-fold increase. The replacement of His72 to Ser/Asn resulted in a dramatic decrease in the catalytic activity, with the k_{cat} value being reduced to ca. 5% and 0.5% of that of the wild-type enzyme, respectively. In contrast, the K_m value was relatively less affected, as shown by the ca. 2-fold and 3-fold increase from H72S and H72N, respectively. Concerns regarding reliability of the enzymatic kinetic results of the His72 mutants may arise due to the heterogeneity of protein caused by the presence of the aforementioned HALS-like species. Such concerns can be eliminated by the following two facts: (a) the HALS-like species is a minor species (<10%), and the relative amount of which barely varies between preps; (b) the ligation of imidazole at the sixth heme coordination is not strong and has shown to be vulnerable to substitution by an active site water in the presence of the substrate. The steady-state kinetic parameters of TDO and the distal histidine variants from other sources are also summarized in Table 2 for comparison.

1-Methyl-L-tryptophan as an Alternative Substrate. Steady-state kinetic assays were performed to investigate the reactivity of 1-Me-L-Trp toward cmTDO. Interestingly, 1-Me-L-Trp was a fairly active substrate for wild-type cmTDO with a k_{cat} value of 8.4 ± 0.4 s^{-1} (Figure 2), which was comparable to

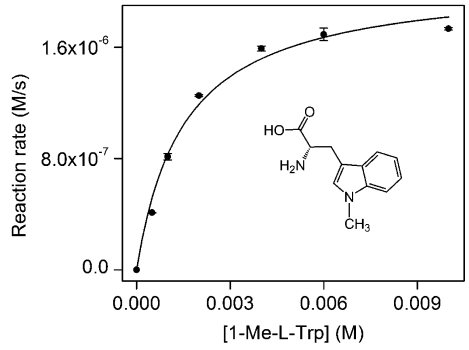

Figure 2. Steady-state kinetic assay of cmTDO with 1-Me-L-Trp as the substrate. The reaction rates were measured at room temperature in the presence of 1 mM L-ascorbate. The final concentration of TDO in the reaction system was 0.25 μM. The solid line is the best fit of experimental data to eq 1. Kinetic parameters were determined from the fitting results.

that of cmTDO with L-Trp as the substrate. The K_m value, however, was elevated by ca. 7-fold to 1.5 ± 0.2 mM upon methylation of the indole nitrogen of the substrate. In contrast, 1-Me-L-Trp was a very poor substrate for the His72 variants of cmTDO. There were no measurable kinetic parameters for these two mutants with 1-Me-L-Trp as the substrate.

Interactions between Exogenous Imidazoles and the Heme Center of cmTDO. Imidazole and its analogues have been widely used as histidine surrogates in chemical rescue experiments on histidine mutants to investigate the functions of active site histidine in many enzyme systems.[52−56] However, they are also potential ligand molecules that have been

extensively used in coordination chemistry studies of model heme complexes and hemoproteins.[57−60] Therefore, caution should be exercised when introducing imidazoles to the reaction systems of heme-dependent enzymes as rescuing reagents.

CmTDO and its variants in the ferric state were incubated with an excess amount (i.e., 50 mM) of different imidazoles (IM, 2MI, and 4MI) in separate experiments, and characterized by UV−vis and EPR spectroscopy. In WT-TDO, there were no changes in the absorption maximum of the Soret band upon addition of imidazoles (Figure S3A of the SI). In Q73F, a subtle red-shift of ∼1 nm in the Soret band was observed in the presence of IM and 4MI but not 2MI (Figure S3B of the SI). In the His72 variants, the red shift became more observable (4−5 nm) upon addition of IM and 4MI, accompanied by a pronounced decrease in the absorption intensity (Figure S3C,D). In contrast, 2MI did not lead to the same phenomenon in either of the His72 mutants with the corresponding UV−vis spectra resembled those of the as-isolated proteins yet with slightly decreased Soret band (Figure S3C,D). Previous studies have demonstrated that direct ligation of imidazoles to the heme iron causes a red shift in the Soret band.[56,59,60] 2MI, however, is not able to effectively ligate to the heme center of TDO, possibly due to steric hindrance caused by the methyl group seated in between the two nitrogen atoms.

Addition of 2MI to cmTDO and the three mutants did not lead to observable changes in the EPR spectra (Figure S4 of the SI), confirming that 2MI is not an effective heme ligand. However, in the presence of IM or 4MI, the high-spin ferric signal in the His72 mutants vanished, with a concurrent increase in the signal of the imidazole-induced HALS-like species described earlier (Figure S4C,D). In contrast, addition of IM or 4MI had relatively less effect on the EPR spectrum of Q73F and almost no influence on the EPR spectrum of WT-TDO (Figure S4A,B).

Chemical Rescue of Enzyme Activity in the His72 Mutants by Exogenous Imidazoles. Kinetic assays were performed on cmTDO and its mutants in the absence and presence of different imidazoles. The order of addition of imidazoles and other assay components did not alter enzymatic reaction rates. In WT-TDO and Q73F, exogenous imidazoles had little effect on the catalytic activity (Figure S5A,B of the SI). In contrast, the presence of 2MI in the reaction system enhanced the reaction rates of both His72 variants, whereas addition of IM or 4MI was not able to contribute as much (Figure S5C,D). Therefore, 2MI was selected as the rescuing reagent for the catalytic activities of the His72 variants.

The His72 mutants adhered to saturation kinetics with respect to the rescuing reagent 2MI (Figure S6 of the SI). By fitting the experimental data to eq 1, the Michaelis−Menten constants for the rescue reagent, which were redefined here as $K_{activation}$, were determined to be 18 ± 3 and 16 ± 2 mM for H72S and H72N, respectively.

The turnover numbers of H72S and H72N at saturating 2MI condition (i.e., 50 mM) were determined to be 3.1 ± 0.2 and 0.23 ± 0.01 s^{-1}, respectively, which are ca. 6- and 4-fold higher than the k_{cat} values determined in the absence of this rescuing reagent (Figure 3 and Table 2). The K_m values for L-Trp were determined as 0.43 ± 0.06 and 0.43 ± 0.04 mM for H72S and H72N in the presence of 2MI, respectively, which were quite similar to those values obtained in the absence of 2MI. Moreover, 2MI was able to rescue the enzymatic activity of the His72 mutants by a ca. 4-fold increase when 1-Me-L-Trp was used as the substrate, while this compound had little effect on WT-TDO and Q73F (Figure S7 of the SI).

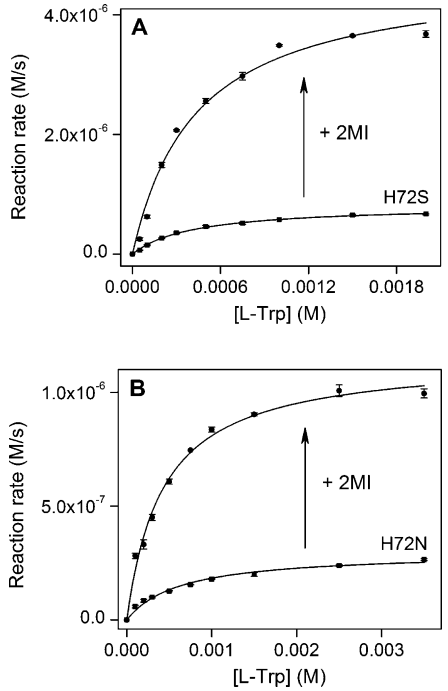

Figure 3. Steady-state kinetic assays of H72S (A) and H72N (B) in the absence (■) and presence (●) of 2MI (50 mM). The reaction rates were measured at room temperature in the presence of 1 mM L-ascorbate. The final concentration of enzyme was 1.5 μM for H72S and 5 μM for H72N. The solid lines are the best fits of experimental data to eq 1.

Stopped-Flow UV−vis Characterization of a Ferryl Species in cmTDO. Previously, we reported a peroxide-mediated enzyme reactivation mechanism of TDO.[35] A Cpd ES-type of ferryl species was identified in the reactivation process and characterized by EPR and Mössbauer spectroscopy.[35] Here, we took advantage of the previous findings to examine the effects of mutation and chemical rescue on this ferryl species. Upon rapid mixing of ferric WT-TDO (UV−vis spectrum: 405, 504, and 539 nm) with H_2O_2 (5 mM), a new heme species with a red-shifted Soret band (414 nm) as well as altered visible bands (526 and 548 nm) was generated in the millisecond time window as measured by stopped-flow UV−vis spectroscopy (Figure 4A) and was assigned as the aforementioned Cpd ES species. Concurrent with the formation of the ferryl species, the charge transfer band around 630 nm was reduced in intensity. The observation of isosbestic points at 461, 514, and 618 nm (Figure 5A and Table 3) suggests that this is a single transition process (from ferric to ferryl TDO). The formation rate of this ferryl species was determined to be 27.2 ± 0.2 s^{-1} by following the decay of the ferric enzyme at its Soret band absorption intensity. Parallel experiments performed in the presence of highly concentrated H_2O_2 (i.e., above 100 mM) revealed the formation of the same type of ferryl species (data not shown). In the reaction between Q73F and H_2O_2 (5 mM), a similar ferryl species with nearly identical optical absorption features (413, 526, and 548 nm) was observed (Figure S8A of the SI). The formation rate of this ferryl species was calculated to be 16.7 ± 0.4 s^{-1} based on the decay of the ferric heme.

dx.doi.org/10.1021/ja304164b | J. Am. Chem. Soc. 2012, 134, 12209−12218

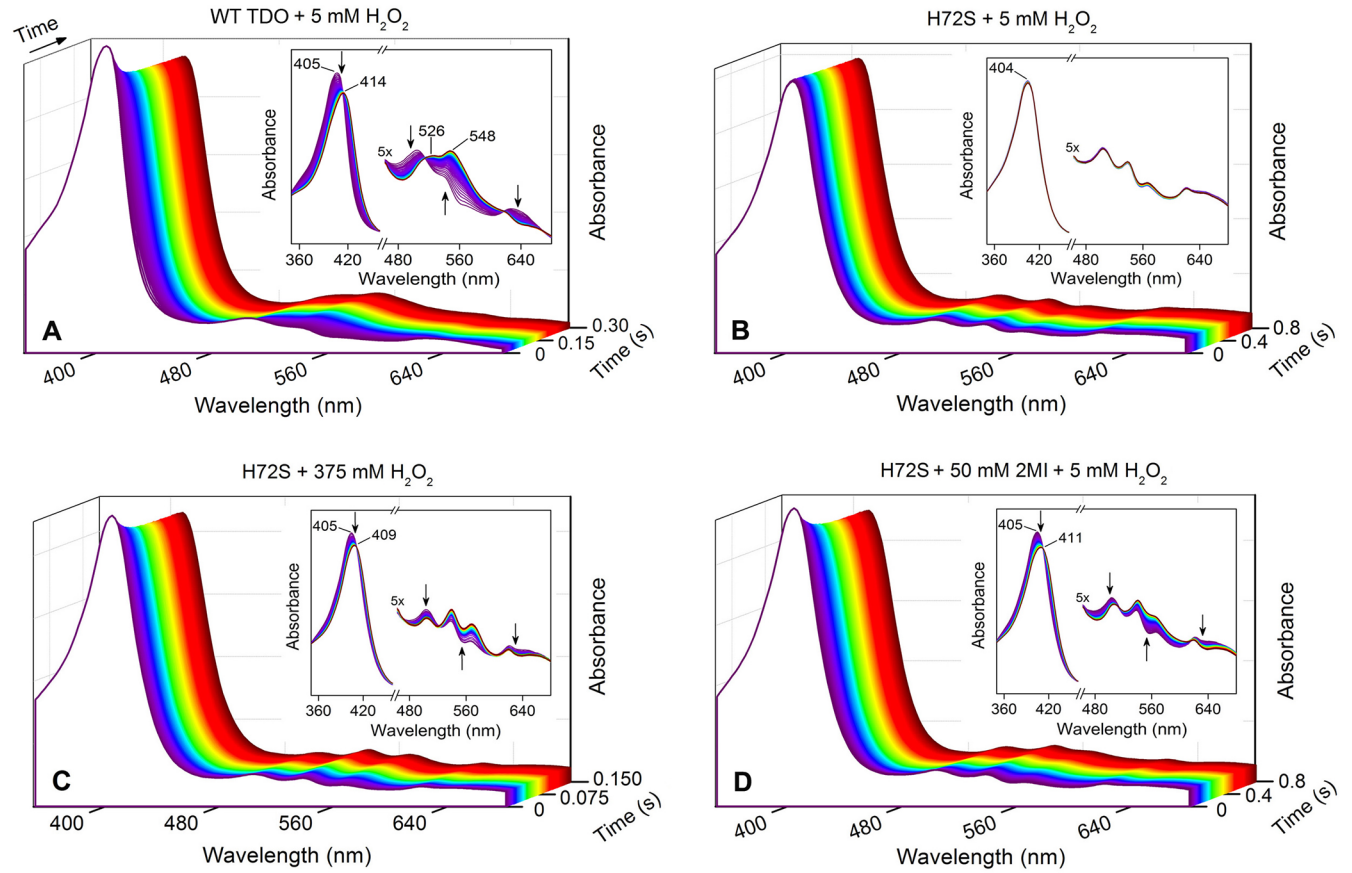

Figure 4. Time-resolved stopped-flow UV−vis spectra (3-D) of the reactions between cmTDO (15 μM) and H_2O_2 at 4 °C. (A) WT-TDO + 5 mM H_2O_2 (0−0.3 s); (B) H72S + 5 mM H_2O_2 (0−0.8 s); (C) H72S + 375 mM H_2O_2 (0−0.15 s); (D) H72S + 5 mM H_2O_2 with 50 mM 2MI in the reaction system (0−0.8 s). The insets are corresponding 2-D expanded views. The arrows indicate the trends of changes in the spectra.

In sharp contrast, no transition intermediates were detected during the reactions between the His72 mutants and peroxide (Figure 4B and Figure S8B of the SI), suggesting the functional importance of His72 in generating or stabilizing the ferryl species in cmTDO. However, in the presence of highly concentrated H_2O_2 (i.e., above 100 mM), the formation of a new species, possibly a ferryl heme species as judged by the spectral features, could be observed in the millisecond time window (Figure 4C and Figure S8C of the SI). The formation rates of this new species generated by 375 mM H_2O_2 were determined to be 53 ± 6 and 15.5 ± 0.3 s^{-1} in H72S and H72N, respectively. At longer time scales, the heme became severely bleached due to the presence of such high concentration of H_2O_2.

Inspired by our chemical rescue results, we introduced 2MI to the stopped-flow experiments with the aim of rescuing the formation of ferryl species from the His72 variants in the presence of less concentrated H_2O_2 (i.e., 5 mM). While no significant changes in the time-resolved spectra were observed during the reaction between H72S and 5 mM H_2O_2, the accumulation of a new species with a red-shifted Soret band (411 nm), altered visible bands, and a reduced charge transfer band, was observed in the same reaction system supplemented with 50 mM 2MI (Figure 4D). Again, this species was assigned as a ferryl species based on the similarity of its spectral features to those of the Cpd ES species from WT-TDO. Similar chemical rescue results were obtained from H72N (Figure S8D of the SI). The formation rates of this rescued ferryl species were calculated to be 7.3 ± 0.1 and 1.4 ± 0.1 s^{-1} for H72S/2MI and H72N/2MI, respectively.

We were able to generate two forms of ferryl species in the His72 mutants via two different strategies. Direct comparison of the time-resolved stopped-flow spectra between these two groups of ferryl species only revealed slight differences, due to the similarity of their redox states and the incomplete accumulation caused by either too much H_2O_2 in the reaction system or relatively low formation rates. Therefore, time-resolved difference spectra were constructed for better comparison and differentiation of the transition processes (from ferric to ferryl) in different reaction systems. Table 3 summarizes the key features of these difference spectra. In the difference spectra of WT-TDO, two negative peaks developed at 493 and 638 nm, and a positive peak at 555 nm with two shoulders at 528 and 598 nm (Figure 5A). In addition, three isosbestic points (461, 514, and 518 nm) were identified for the transition process. Q73F showed almost the same difference spectra (Figure S9A of the SI). The putative ferryl species rescued by 2MI from the His72 variants presented very similar difference spectra with nearly identical isosbestic points (Figure 5C and Figure S9C of the SI). However, the putative ferryl species accumulating in the presence of highly concentrated H_2O_2 showed quite different difference spectra (Figure 5B and Figure S9B of the SI) as compared to the ferryl species from WT-TDO and Q73F. The differences were outlined by significant alterations in the absorption maxima of both the positive and negative peaks on the spectra as well as the positions of the isosbestic points (Table 3).

dx.doi.org/10.1021/ja304164b | J. Am. Chem. Soc. 2012, 134, 12209−12218

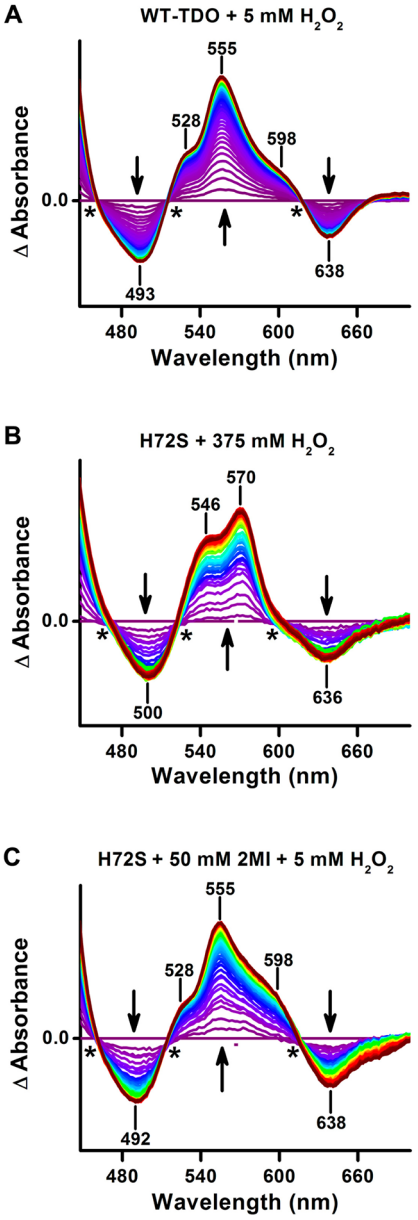

Figure 5. Time-resolved stopped-flow UV−vis difference spectra of the reactions between cmTDO (15 μM) and H_2O_2 at 4 °C. (A) WT-TDO + 5 mM H_2O_2 (0−0.3 s); (B) H72S + 375 mM H_2O_2 (0−0.15 s); (C) H72S + 5 mM H_2O_2 with 50 mM 2MI in the reaction system (0−0.8 s). The arrows indicate the trends of changes in the spectra. The "*" symbol indicates the isosbestic points identified in the visible region.

DISCUSSION

The Role of the Distal Histidine. We propose a dual function for the distal His72 in cmTDO: (a) facilitating substrate binding through an H-bonding interaction while protecting the heme center from nonproductive binding of exogenous small ligand molecules (i.e., imidazole and its analogs) via steric effect, and (b) contributing to the chemical catalysis process by providing H-bonding interactions to the oxygen-bound heme intermediates including the putative ferryl intermediate that was proposed in the dioxygenase catalytic cycle.[31,33,61]

The first function is supported by the kinetic assays with 1-Me-L-Trp as the substrate and the spectroscopic characterizations of binding events with exogenous imidazoles. Additional support is provided by the biochemical studies on the Q73F mutant. The second function is proposed based on our chemical rescue experiments on the distal histidine variants of the enzymatic activity in both the dioxygenase catalytic cycle and the formation of a peroxide-induced ferryl species with 2MI as the rescuing reagent. The proposed H-bonding interaction provided by the distal histidine would contribute to stabilization of the putative ferryl intermediate and thus help boost the catalytic efficiency. Detailed discussions on the proposed functions of the distal histidine are presented below.

Table 3. Optical Absorption Features Identified in the Time-Resolved Difference Spectra during the Peroxide-Induced Transition Process from Ferric to Ferryl TDO

	positive peak (nm)			negative peak (nm)		isosbestic point (nm)		
protein	#1	#2	#3	#1	#2	#1	#2	#3
WT-TDO	528	555	598	493	638	461	514	618
Q73F	528	555	598	494	638	461	514	618
H72S[a]	546	570		500	636	471	522	602
H72N[a]	546	570		501	636	472	521	602
H72S + 2MI[b]	528	555	598	492	638	461	514	618
H72N + 2MI[b]	528	555	598	494	638	464	514	618

[a]Highly concentrated H_2O_2 (i.e., 375 mM) was used to generated the putative ferryl species in this set of experiments. [b]The experiments were performed in the presence of 50 mM 2MI.

The Effects of Site-Directed Mutagenesis. Upon replacement of His72 with Ser/Asn, a significant decrease in the catalytic activity was observed, with a more pronounced effect on k_{cat} than K_m. Distal histidine variants from other sources also presented declines in the enzymatic activity at different degrees (Table 2). The notable decrease in activity of the His72 mutants appears to result from the absence of the imidazole side chain of His72 rather than structural changes in the active site, since spectroscopic characterizations of the mutant proteins revealed no substantial changes.

Exogenous imidazole was not able to coordinate to the heme iron of wild-type cmTDO. In contrast, the same molecule was allowed to directly ligate to the heme center after substitution of His72 to Ser/Asn and generate a HALS-like species at the expense of the resting high-spin ferric species. Interestingly, it was demonstrated by Sono and colleagues that imidazole can coordinate to the heme center of IDO, which has a serine residue occupying the analogous distal position of His72, and cause a distinctive red-shift of the Soret band.[50] They also observed a HALS-like species with similar EPR parameters (g = 2.86, 2.28, and 1.60) from as-isolated IDO, which became the major species in the EPR spectrum upon addition of exogenous imidazole.[50] A similar HALS-like species (g = 2.94, 2.25, and 1.50) was reported in as-isolated hIDO.[48] Upon addition of the L-Trp, the amount of this species decreased to generate the substrate-induced hydroxide-bound low-spin heme species,[48] resembling the phenomenon observed in the His72 mutants in this study. Taken together, it can be concluded that possibly via steric hindrance, the distal His72 can efficiently shield the heme center of cmTDO from nonproductive binding of exogenous small ligand molecules, such as imidazole and its analogs. Moreover, Basran et al. reported the existence of the same type of HALS-like species (g = 2.8, 2.3, and 1.6) in as-isolated hTDO,[45] suggesting that imidazole is capable of coordinating

dx.doi.org/10.1021/ja304164b | J. Am. Chem. Soc. 2012, 134, 12209−12218

to the heme center of hTDO even in the presence of the distal histidine. Therefore, TDO proteins from different sources might possess slightly different heme microenvironments and active-site architectures.

In contrast to the His72 mutants, Q73F inherited the majority of the key features from WT-TDO, including spectroscopic properties and enzymatic reactivity without distinctive alterations. Therefore, with the distal histidine present, most of the biochemical properties of the enzyme are well-conserved. However, this variant differed from the native enzyme in certain aspects: the replacement of Gln73 introduced the most distinct influence on the K_m value (a ca. 5-fold increase); the mutation also moderately increased the heme accessibility to allow coordination of exogenous imidazole. Thus, the physical position of His72 is very important in maintaining the biological functions of the cmTDO.

1-Methyl-L-Trp as an Alternative Substrate. It has been previously reported by Raven and colleagues that 1-Me-L-Trp is a slow substrate for hIDO as well as the distal histidine variants of hTDO (H76A) and xcTDO (H55A and H55S) but is inactive to the wild-type TDO enzymes.[28] This finding has important mechanistic implications. Under the assumption that 1-Me-L-Trp and L-Trp react by the same mechanism, it is suggested that deprotonation of the indole NH group of the substrate is not an essential step for catalysis.[28] In the present study, 1-Me-L-Trp is demonstrated for the first time to be an active substrate to a wild-type TDO enzyme with comparable reactivity to that of L-Trp. This finding adds one more piece of direct and strong experimental evidence to the above-mentioned notion, i.e., the catalytic cycle of TDO is not initiated by deprotonation of the substrate indole group, which has also been supported by some recent computational studies.[30−33]

With a methyl group attached to the indole nitrogen, 1-Me-L-Trp is shown to present a significantly altered K_m value. The nearly 7-fold increase in K_m reflects a lower affinity of this substrate analogue to the enzyme, which can be attributed to the loss of the H-bonding interaction between the imidazole group of His72 and the indole NH group of the substrate.

Chemical Rescue for the Catalytic Activity. The distal histidine was mutated to alanine and serine by several laboratories in the past.[25−27] This is the first time that the diminished catalytic activity, due to site-directed mutation, has been shown to be recoverable to an appreciable degree by a histidine analogue (i.e., 2MI). In contrast, both IM and 4MI failed to show a comparable ability to stimulate the enzymatic activity of the His72 mutants, presumably due to the fact that their chemical rescue effect was nullified by the inhibition effect caused by heme coordination. Spectroscopic studies demonstrated that IM and 4MI are able to coordinate to the heme center of the His72 variants to produce hexa-coordinated heme species, whereas 2MI cannot directly ligate to the heme iron. It should be noted that while 2MI is able to cause an appreciable increase in the k_{cat} values, this compound only minutely altered the K_m values. Thus, the chemical rescue effect was mainly focused on the chemical catalytic steps rather than the substrate binding step. This suggests that the enzyme-bound 2MI molecules are less likely to play a role in assisting substrate binding; rather, they are able to participate in the chemical catalytic steps in a way that mimics the role of His72.

Chemical Rescue Effect on Ferryl Species and the Proposed Role of His72 in Catalysis. TDO and IDO are generally thought to share similar catalytic strategies. An Fe(IV)=O intermediate (Cpd II-type) has been observed from IDO and characterized by resonance Raman spectroscopy.[31] Such a ferryl intermediate has not yet been captured in TDO, presumably because the catalytic reaction rate is much faster. However, it has been proposed as one of the key intermediates in the dioxygenase catalytic cycle of TDO in recent computational studies.[31,33] Previously, we have identified and characterized a peroxide-mediated ferryl species (Cpd ES-type) in TDO via EPR and Mössbauer spectroscopy during the enzyme reactivation cycle, demonstrating an alternative way to generate the ferryl species in TDO.[35]

While the ferryl species was observed from WT-TDO via stopped-flow UV−vis spectroscopy in peroxide reaction, no such intermediate could be identified during the reaction between His72 variants and H_2O_2 under the same condition. By significantly increasing the H_2O_2 concentration, we were able to generate a different ferryl species from the His72 variants with disparate spectral features as revealed by the difference spectra. It has been shown that the visible bands of ferryl heme are sensitive to the changes in the electronic structure of the Fe(IV)=O moiety. For example, the visible bands of ferryl heme in myoglobin and hemoglobin have been demonstrated to be susceptible to the protonation state.[62] Herein, we propose that the differences in the spectral features between the ferryl species from WT-TDO and the His72 mutants resulted from the loss of H-bonding interaction between the distal histidine and the Fe(IV)-oxo group. The proposed H-bonding interaction plays an important structural role in stabilizing the Fe(IV)=O moiety of the ferryl species in cmTDO, as suggested by the requirement of such high concentration of H_2O_2 for the occurrence of accumulation of the ferryl species in the His72 mutants. Our previous Mössbauer spectroscopic characterization revealed a unique quadrupole splitting (ΔE_Q) value (1.755 mm/s determined at pH 7.4) for the peroxide-mediated ferryl species from WT-TDO,[35] which lies in between the ranges for protonated Fe(IV)−OH species (2.0−2.5 mm/s)[63] and unprotonated Fe(IV)=O species (1.0−1.6 mm/s).[63−67] Subsequent DFT calculations indicated that the unusual ΔE_Q value originates from H-bonding interaction provided by the protein matrix,[35] and His72 is an ideal candidate for providing the proposed H-bonding interaction with the Fe(IV)-oxo group.

The spectral similarities between the ferryl species from WT-TDO and those rescued by 2MI from the His72 variants suggest that these two groups of ferryl species structurally resemble each other. Therefore, by substituting for His72, 2MI is able to rescue the accumulation of the same Cpd ES-type of ferryl species as that from WT-TDO in both His72 mutants at relatively low H_2O_2 concentration (Scheme 2). However, due to its exogenous nature, the binding occupancy and the effective binding ratio of 2MI are expected to be limited, hampering its rescuing effect, as suggested by the relatively low formation rate of the rescued ferryl species.

■ CONCLUSIONS

Scheme 3 illustrates the proposed role of His72 during the dioxygenase reaction of cmTDO. Other than participating in the initial L-Trp binding process and properly positioning it at the active site, His72 is proposed to stabilize the oxygen-bound heme intermediates during the subsequent catalytic steps. The key catalytic intermediate is a Cpd II-type of ferryl species, which is similar to, but not the same as the Cpd ES species

Scheme 2. Proposed Role of His72 in Stabilizing the Ferryl Species in cmTDO during Peroxide Reaction[a]

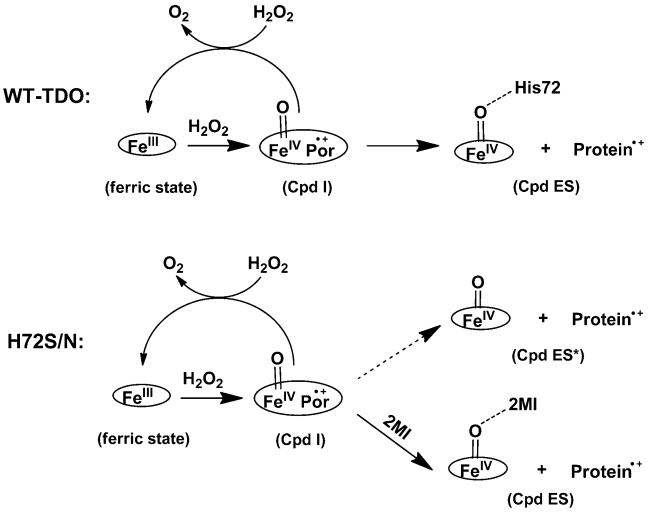

[a]The catalase-like cycle of TDO has been reported previously.[35] "Cpd ES" differs from "Cpd ES*" by an additional H-bonding interaction to either the His72 residue or 2MI. The accumulation of "Cpd ES*" can be observed only in the presence of highly concentrated H_2O_2 (i.e., over 100 mM).

Scheme 3. Proposed Role of His72 in Catalysis during the Dioxygenase Reaction Cycle of cmTDO[a]

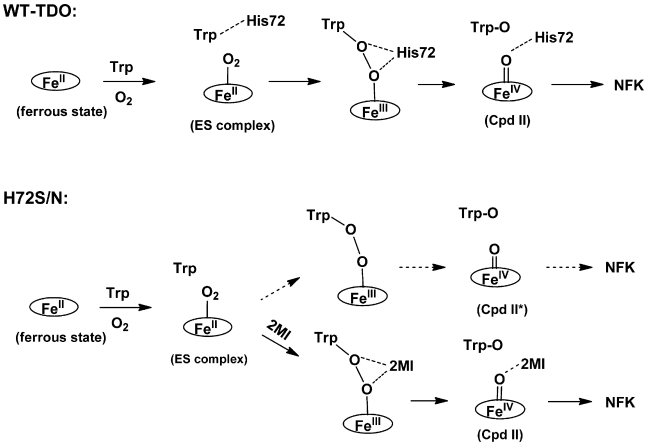

[a]"Cpd II" differs from "Cpd II*" by an additional H-bonding interaction to either the His72 residue or 2MI.

observed in the peroxide-mediated enzyme reactivation pathway, which possess an additional oxidizing equivalent stored as a protein-based radical. However, oxidation of L-Trp by the Fe(IV)=O moiety and by the protein radical are separated reactions in the enzyme reactivation mechanism.[35] Therefore, the proposed Cpd II species has been implicated in the later stage of the enzyme reactivation pathway. The data presented in this work show that the properties of the ferryl species in cmTDO are dependent on the presence of the distal His72. In its absence, 2MI can effectively play the part played by His72, thus rescuing the enzymatic activity.

■ ASSOCIATED CONTENT

Supporting Information

Table S1 and Figures S1–S9. This material is available free of charge via the Internet at http://pubs.acs.org.

■ AUTHOR INFORMATION

Corresponding Author

Feradical@gsu.edu (Aimin Liu)

Notes

The authors declare no competing financial interest.

*Notes from the manufacturer: 1-Me-L-Trp was synthesized from a route that does not utilize L-Trp as the starting material. There were no side reactions which introduces L-Trp as one of the impurities.

■ ACKNOWLEDGMENTS

This work was supported by NSF Grant MCB-0843537 and Georgia Cancer Coalition Distinguished Scholar Program (A.L.). We thank Rong Fu for her efforts in the initial stage of characterization of the His72 variants and C. Ian Davis for manuscript editing and helpful discussions.

■ REFERENCES

(1) Collman, J. P.; Brauman, J. I.; Halbert, T. R.; Suslick, K. S. *Proc. Natl. Acad. Sci. U. S. A.* **1976**, *73*, 3333–3337.

(2) Stone, T. W.; Darlington, L. G. *Nat. Rev. Drug Discov.* **2002**, *1*, 609–620.

(3) Schwarcz, R. *Curr. Opin. Pharmacol.* **2004**, *4*, 12–17.

(4) Guillemin, G. J.; Meininger, V.; Brew, B. J. *Neurodegener. Dis.* **2005**, *2*, 166–176.

(5) Guillemin, G. J.; Brew, B. J. *Redox Rep.* **2002**, *7*, 199–206.

(6) Yamamoto, S.; Hayaishi, O. *Methods Enzymol.* **1970**, *17*, 434–438.

(7) Kurnasov, O.; Goral, V.; Colabroy, K.; Gerdes, S.; Anantha, S.; Osterman, A.; Begley, T. P. *Chem. Biol.* **2003**, *10*, 1195–1204.

(8) Magni, G.; Amici, A.; Emanuelli, M.; Raffaelli, N.; Ruggieri, S. *Adv. Enzymol. Relat. Areas Mol. Biol.* **1999**, *73*, 135–182.

(9) Tanaka, T.; Knox, W. E. *J. Biol. Chem.* **1959**, *234*, 1162–1170.

(10) Takikawa, O. *Biochem. Biophys. Res. Commun.* **2005**, *338*, 12–19.

(11) Paglino, A.; Lombardo, F.; Arca, B.; Rizzi, M.; Rossi, F. *Insect Biochem. Mol. Biol.* **2008**, *38*, 871–876.

(12) Li, J. S.; Han, Q.; Fang, J.; Rizzi, M.; James, A. A.; Li, J. *Arch. Insect. Biochem. Physiol.* **2007**, *64*, 74–87.

(13) Colabroy, K. L.; Begley, T. P. *J. Bacteriol.* **2005**, *187*, 7866–7869.

(14) Hayaishi, O. *Protein Sci.* **1993**, *2*, 472–475.

(15) Hirata, F.; Hayaishi, O. *Biochem. Biophys. Res. Commun.* **1972**, *47*, 1112–1119.

(16) Shimizu, T.; Nomiyama, S.; Hirata, F.; Hayaishi, O. *J. Biol. Chem.* **1978**, *253*, 4700–4706.

(17) Hayaishi, O. *J. Biochem.* **1976**, *79*, 13–21.

(18) Zhang, Y.; Kang, S. A.; Mukherjee, T.; Bale, S.; Crane, B. R.; Begley, T. P.; Ealick, S. E. *Biochemistry* **2007**, *46*, 145–155.

(19) Sugimoto, H.; Oda, S.; Otsuki, T.; Hino, T.; Yoshida, T.; Shiro, Y. *Proc. Natl. Acad. Sci. U. S. A.* **2006**, *103*, 2611–2616.

(20) Forouhar, F.; Anderson, J. L.; Mowat, C. G.; Vorobiev, S. M.; Hussain, A.; Abashidze, M.; Bruckmann, C.; Thackray, S. J.; Seetharaman, J.; Tucker, T.; Xiao, R.; Ma, L. C.; Zhao, L.; Acton, T. B.; Montelione, G. T.; Chapman, S. K.; Tong, L. *Proc. Natl. Acad. Sci. U. S. A.* **2007**, *104*, 473–478.

(21) Sono, M.; Roach, M. P.; Coulter, E. D.; Dawson, J. H. *Chem. Rev.* **1996**, *96*, 2841–2888.

(22) Thackray, S. J.; Mowat, C. G.; Chapman, S. K. *Biochem. Soc. Trans.* **2008**, *36*, 1120–1123.

(23) Leeds, J. M.; Brown, P. J.; Mcgeehan, G. M.; Brown, F. K.; Wiseman, J. S. *J. Biol. Chem.* **1993**, *268*, 17781–17786.

(24) Hamilton, G. A. *Adv. Enzymol. Relat. Areas Mol. Biol.* **1969**, *32*, 55–96.

(25) Thackray, S. J.; Bruckmann, C.; Anderson, J. L. R.; Campbell, L. P.; Xiao, R.; Zhao, L.; Mowat, C. G.; Forouhar, F.; Tong, L.; Chapman, S. K. *Biochemistry* **2008**, *47*, 10677–10684.

(26) Batabyal, D.; Yeh, S.-R. *J. Am. Chem. Soc.* **2009**, *131*, 3260−3270.
(27) Fukumura, E.; Sugimoto, H.; Misumi, Y.; Ogura, T.; Shiro, Y. *J. Biochem.* **2009**, *145*, 505−515.
(28) Chauhan, N.; Thackray, S. J.; Rafice, S. A.; Eaton, G.; Lee, M.; Efimov, I.; Basran, J.; Jenkins, P. R.; Mowat, C. G.; Chapman, S. K.; Raven, E. L. *J. Am. Chem. Soc.* **2009**, *131*, 4186−4187.
(29) Davydov, R. M.; Chauhan, N.; Thackray, S. J.; Anderson, J. L. R.; Papadopoulou, N. D.; Mowat, C. G.; Chapman, S. K.; Raven, E. L.; Hoffman, B. M. *J. Am. Chem. Soc.* **2010**, *132*, 5494−5500.
(30) Chung, L. W.; Li, X.; Sugimoto, H.; Shiro, Y.; Morokuma, K. *J. Am. Chem. Soc.* **2008**, *130*, 12299−12309.
(31) Lewis-Ballester, A.; Batabyal, D.; Egawa, T.; Lu, C.; Lin, Y.; Marti, M. A.; Capece, L.; Estrin, D. A.; Yeh, S.-R. *Proc. Natl. Acad. Sci. U. S. A.* **2009**, *106*, 17371−17376.
(32) Capece, L.; Lewis-Ballester, A.; Batabyal, D.; Di Russo, N.; Yeh, S.-R.; Estrin, D. A.; Marti, M. A. *J. Biol. Inorg. Chem.* **2010**, *15*, 811−823.
(33) Chung, L. W.; Li, X.; Sugimoto, H.; Shiro, Y.; Morokuma, K. *J. Am. Chem. Soc.* **2010**, *132*, 11993−12005.
(34) Chauhan, N.; Basran, J.; Efimov, I.; Svistunenko, D. A.; Seward, H. E.; Moody, P. C. E.; Raven, E. L. *Biochemistry* **2008**, *47*, 4761−4769.
(35) Fu, R.; Gupta, R.; Geng, J.; Dornevil, K.; Wang, S.; Zhang, Y.; Hendrich, M. P.; Liu, A. *J. Biol. Chem.* **2011**, *286*, 26541−26554.
(36) Gupta, R.; Fu, R.; Liu, A.; Hendrich, M. P. *J. Am. Chem. Soc.* **2010**, *132*, 1098−1109.
(37) Ishimura, Y.; Nozaki, M.; Hayaishi, O.; Nakamura, T.; Tamura, M.; Yamazaki, I. *J. Biol. Chem.* **1970**, *245*, 3593−3602.
(38) Tsai, A. L.; Kulmacz, R. J.; Wang, J. S.; Wang, Y.; Vanwart, H. E.; Palmer, G. *J. Biol. Chem.* **1993**, *268*, 8554−8563.
(39) Ikeda-Saito, M.; Iizuka, T. *Biochim. Biophys. Acta* **1975**, *393*, 335−342.
(40) Gadsby, P. M. A.; Thomson, A. J. *J. Am. Chem. Soc.* **1990**, *112*, 5003.
(41) Walker, F. A. *Chem. Rev.* **2004**, *104*, 589−615.
(42) Walker, F. A. *Coord. Chem. Rev.* **1999**, *185*−*6*, 471−534.
(43) Zoppellaro, G.; Bren, K. L.; Ensign, A. A.; Harbitz, E.; Kaur, R.; Hersleth, H.-P.; Ryde, U.; Hederstedt, L.; Andersson, K. K. *Biopolymers* **2009**, *91*, 1064−1082.
(44) Chen, Y.; Naik, S. G.; Krzystek, J.; Shin, S.; Nelson, W. H.; Xue, S.; Yang, J. J.; Davidson, V. L.; Liu, A. *Biochemistry* **2012**, *51*, 1586−1597.
(45) Basran, J.; Rafice, S. A.; Chauhan, N.; Efimov, I.; Cheesman, M. R.; Ghamsari, L.; Raven, E. L. *Biochemistry* **2008**, *47*, 4752−4760.
(46) Batabyal, D.; Yeh, S.-R. *J. Am. Chem. Soc.* **2007**, *129*, 15690−15701.
(47) Uchida, K.; Shimizu, T.; Makino, R.; Sakaguchi, K.; Iizuka, T.; Ishimura, Y.; Nozawa, T.; Hatano, M. *J. Biol. Chem.* **1983**, *258*, 2526−2533.
(48) Papadopoulou, N. D.; Mewies, M.; McLean, K. J.; Seward, H. E.; Svistunenko, D. A.; Munro, A. W.; Raven, E. L. *Biochemistry* **2005**, *44*, 14318−14328.
(49) Terentis, A. C.; Thomas, S. R.; Takikawa, O.; Littlejohn, T. K.; Truscott, R. J. W.; Armstrong, R. S.; Yeh, S.-R.; Stocker, R. *J. Biol. Chem.* **2002**, *277*, 15788−15794.
(50) Sono, M.; Dawson, J. H. *Biochim. Biophys. Acta* **1984**, *789*, 170−187.
(51) Yonetani, T.; Anni, H. *J. Biol. Chem.* **1987**, *262*, 9547−9554.
(52) An, H. Q.; Tu, C. K.; Duda, D.; Montanez-Clemente, I.; Math, K.; Laipis, P. J.; McKenna, R.; Silverman, D. N. *Biochemistry* **2002**, *41*, 3235−3242.
(53) Lehoux, I. E.; Mitra, B. *Biochemistry* **1999**, *38*, 9948−9955.
(54) Wilks, A.; Sun, J.; Loehr, T. M.; Ortiz de Montellano, P. R. *J. Am. Chem. Soc.* **1995**, *117*, 2925−2926.
(55) Ghanem, M.; Gadda, G. *Biochemistry* **2005**, *44*, 893−904.
(56) Newmyer, S. L.; Ortiz de Montellano, P. R. *J. Biol. Chem.* **1996**, *271*, 14891−14896.
(57) Salerno, J. C.; Leigh, J. S. *J. Am. Chem. Soc.* **1984**, *106*, 2156−2159.
(58) Migita, C. T.; Iwaizumi, M. *J. Am. Chem. Soc.* **1981**, *103*, 4378−4381.
(59) Berka, V.; Palmer, G.; Chen, P. F.; Tsai, A. L. *Biochemistry* **1998**, *37*, 6136−6144.
(60) Dawson, J. H.; Sono, M. *Chem. Rev.* **1987**, *87*, 1255−1276.
(61) Efimov, I.; Basran, J.; Thackray, S. J.; Handa, S.; Mowat, C. G.; Raven, E. L. *Biochemistry* **2011**, *50*, 2717−2724.
(62) Silaghi-Dumitrescu, R.; Reeder, B. J.; Nicholls, P.; Cooper, C. E.; Wilson, M. T. *Biochem. J.* **2007**, *403*, 391−395.
(63) Green, M. T.; Dawson, J. H.; Gray, H. B. *Science* **2004**, *304*, 1653−1656.
(64) Behan, R. K.; Hoffart, L. M.; Stone, K. L.; Krebs, C.; Green, M. T. *J. Am. Chem. Soc.* **2006**, *128*, 11471−11474.
(65) Stone, K. L.; Hoffart, L. M.; Behan, R. K.; Krebs, C.; Green, M. T. *J. Am. Chem. Soc.* **2006**, *128*, 6147−6153.
(66) Horner, O.; Mouesca, J. M.; Solari, P. L.; Orio, M.; Oddou, J. L.; Bonville, P.; Jouve, H. M. *J. Biol. Inorg. Chem.* **2007**, *12*, 509−525.
(67) Behan, R. K.; Green, M. T. *J. Inorg. Biochem.* **2006**, *100*, 448−459.

Supporting Information

Chemical Rescue of the Distal Histidine Mutants of Tryptophan 2,3-Dioxygenase

Jiafeng Geng, Kednerlin Dornevil, and Aimin Liu[*]

Department of Chemistry & Center for Diagnostics and Therapeutics, Georgia State University, 161 Jesse Hill Jr. Drive, Atlanta, GA 30303

List of Supporting Table and Figures

Table S1. Optical absorption maxima of cmTDO in the absence and presence of L-Trp

Sample	Ferric form (nm)	Ferrous form (nm)
WT-TDO	405, 504, 539	432, 553, 585
WT-TDO + L-Trp	406, 504, 539	432, 552, 585
Q73F	405, 503, 539	432, 554, 586
Q73F + L-Trp	406, 502, 539	432, 554, 586
H72S	404, 503, 537	428, 555, 583
H72S+ L-Trp	405, 503, 537	428, 555, 583
H72N	403, 501, 537	428, 553, 584
H72N + L-Trp	404, 501, 537	428, 553, 583

Figure S1. Optical absorption spectra of cmTDO (10 μM) in the absence and presence of L-Trp (10 mM). Black: ferric TDO; Red: ferric TDO + L-Trp; Green: ferrous TDO; Blue: ferrous TDO + L-Trp. The insets are the expanded views of the visible bands.

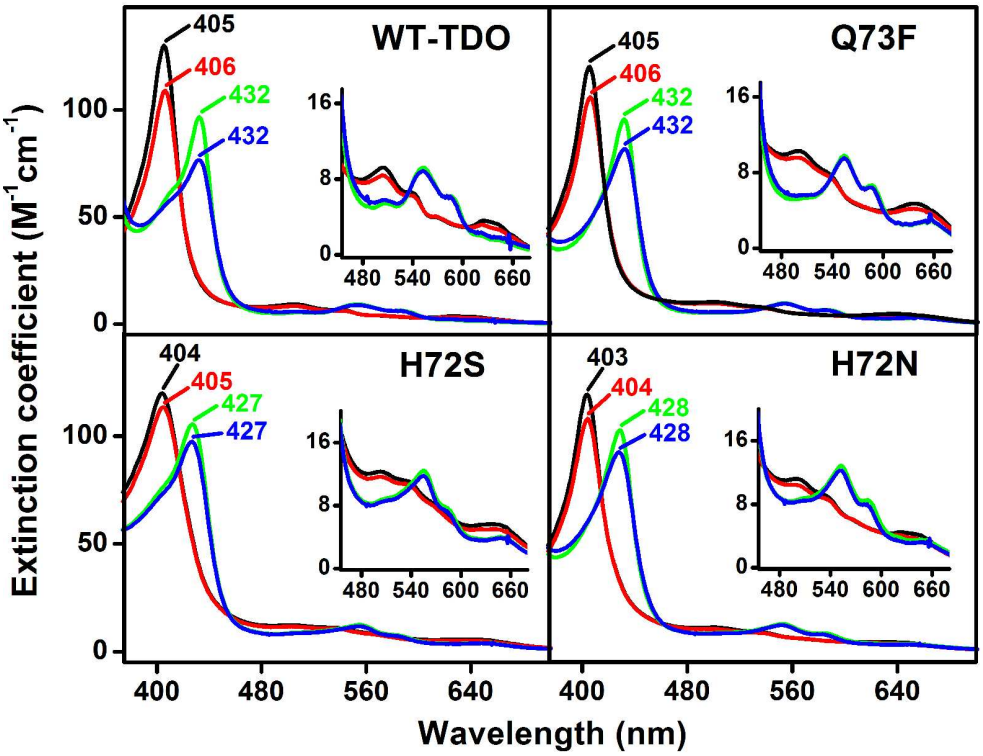

Figure S2. pH effect on the optical absorption spectra of cmTDO and its mutants (8 μM). (A) WT-TDO, (B) Q73F, (C) H72S, (D) H72N. This experiment was performed over the pH range from 6 (black) to 11 (green) in multi-component buffer solutions containing 50 mM Tris, 50 mM MOPS, and 50 mM glycine. The pH difference between each two adjacent data set is 1 unit. The arrows indicate the trends of changes in the spectra. The insets present the changes in the Soret band absorption intensity as a function of pH. The solid lines are the best fits of the experimental data to one-proton titration curves.

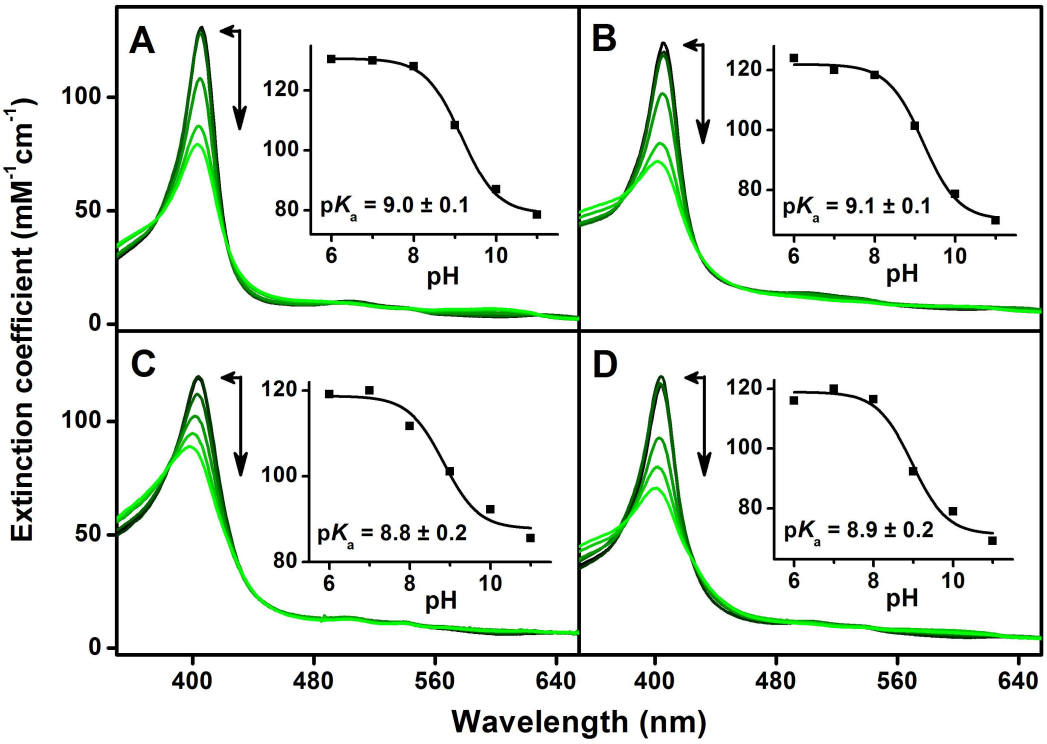

Figure S2 shows that upon increasing pH, the Soret bands in cmTDO and its mutants decreased in intensity and slightly blue-shifted. Moderate alterations in the visible bands were also observed. The observed isosbestic points in the spectra suggested that only two components are responsible for the pH effect. Therefore, the changes in the Soret band absorption intensity for each protein were fitted to a one-proton titration curve as a function of pH. Even though the origin of the pK_a values obtained from the fitting results is not clear at this stage, it can still be concluded that the mutation did not have a pronounced effect on the electrostatic properties of the heme centers in cmTDO.

Figure S3. Optical absorption spectra of the Soret band in ferric cmTDO (8 μM) in the absence and presence of exogenous imidazoles (50 mM). (A) WT-TDO, (B) Q73F, (C) H72S, (D) H72N. Black: as-isolated; Red: with 2MI; Green: with IM; Blue: with 4MI.

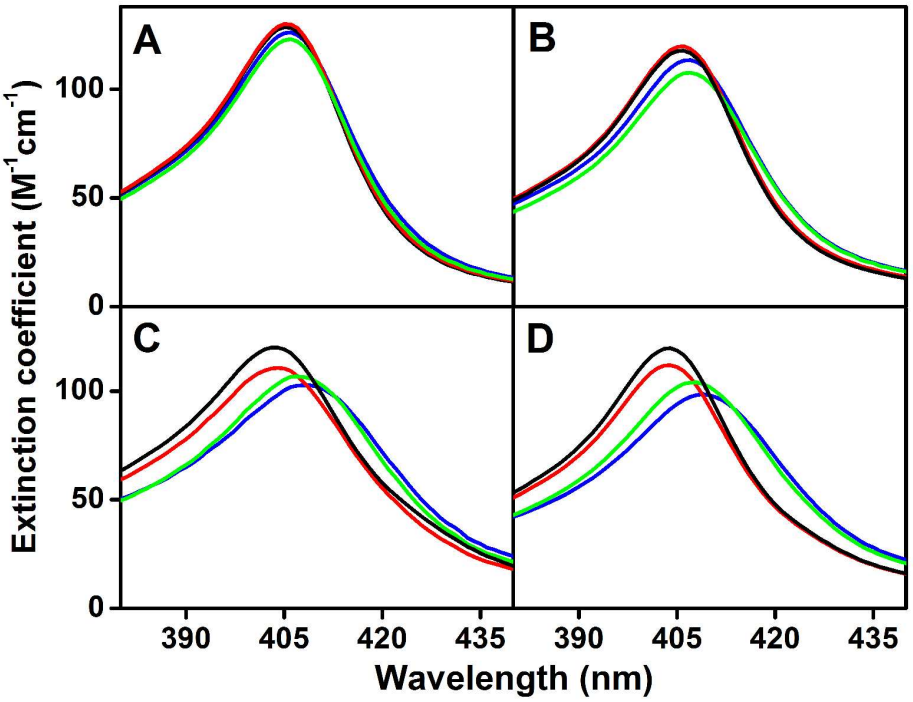

Figure S4. EPR spectra of cmTDO (200 μM heme concentration) in the absence and presence of exogenous imidazole and its analogs (50 mM). (A) WT-TDO, (B) Q73F, (C) H72S, (D) H72N. Black: as-isolated; Red: with 2MI; Green: with IM; Blue: with 4MI. Experimental conditions: temperature, 10 K; microwave frequency, 9.65 GHz; microwave power, 3 mW.

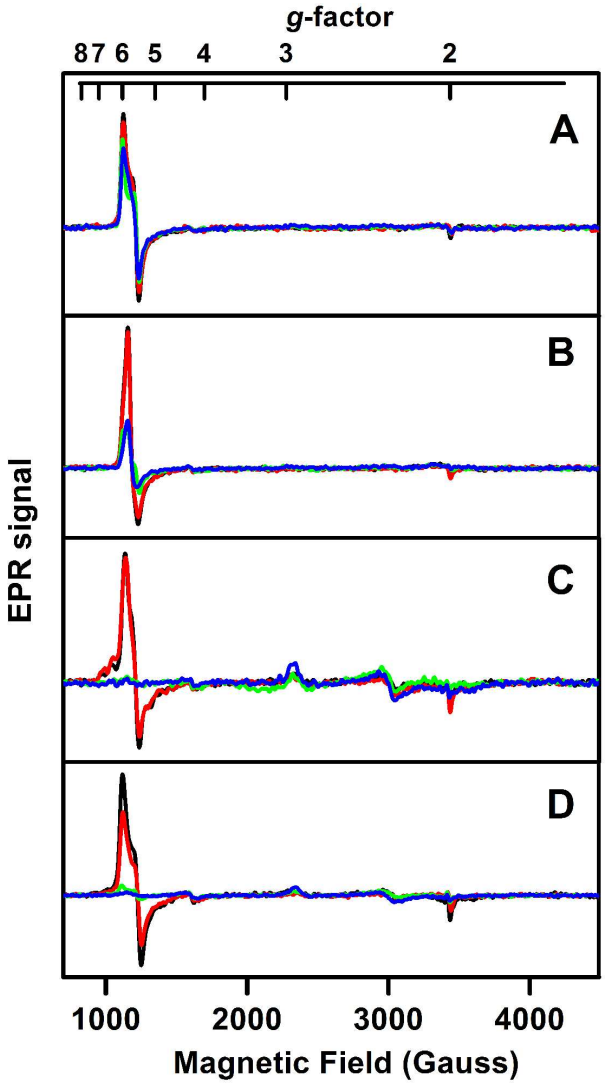

Figure S5. Comparison of enzymatic activities of cmTDO in the absence and presence of exogenous imidazoles. (A) WT-TDO, (B) Q73F, (C) H72S, (D) H72N. Formation of the product – NFK was monitored by the increase of absorbance at 321 nm. The kinetic traces were obtained in the presence of 1 mM L-Trp and 1 mM L-ascorbate, with no exogenous imidazoles (black), 50 mM 2MI (red), 50 mM IM (green), or 50 mM 4MI (blue). The final concentration of enzyme in the reaction system was 0.15 μM for WT-TDO, 0.2 μM for Q73F, 1.5 μM for H72S and 5 μM for H72N. For each individual trace, the absorbance at the starting point was subtracted over the whole time course to correct for background.

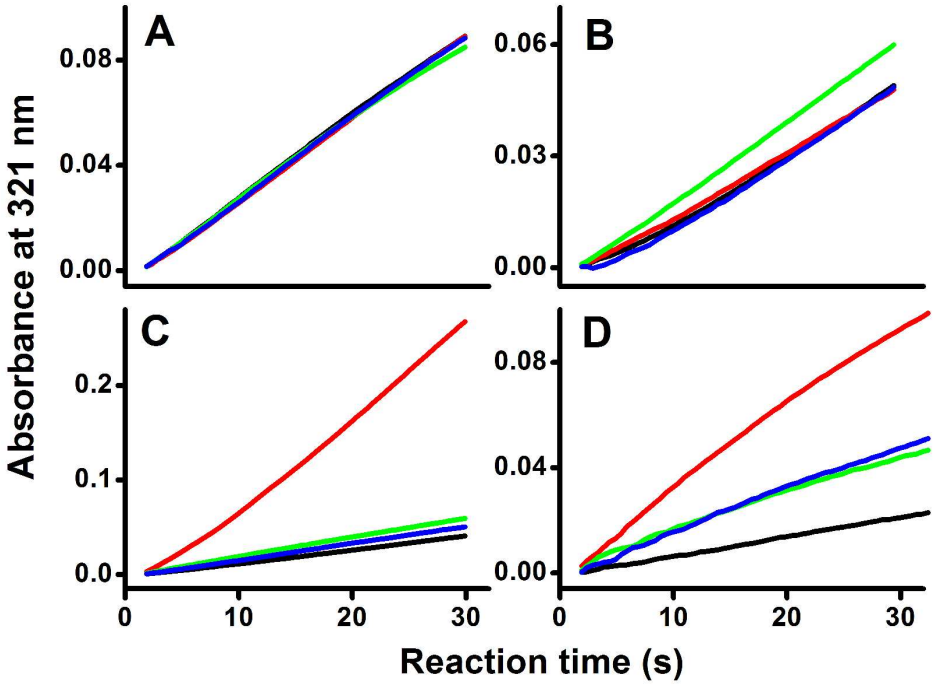

Figure S6. Rescued catalytic activities of H72S (A) and H72N (B) as a function of 2MI concentration. The reaction rates were measured at room temperature in the presence and absence different concentrations of 2MI, with 1 mM L-ascorbate and 1mM L-Trp in the reaction systems. The final concentration of enzyme was 1.5 μM for H72S and 5 μM for H72N. The rescued catalytic activity is the difference between the reaction rates determined in the presence and absence of 2MI. The solid lines are the best fits of experimental data to Eq. 1.

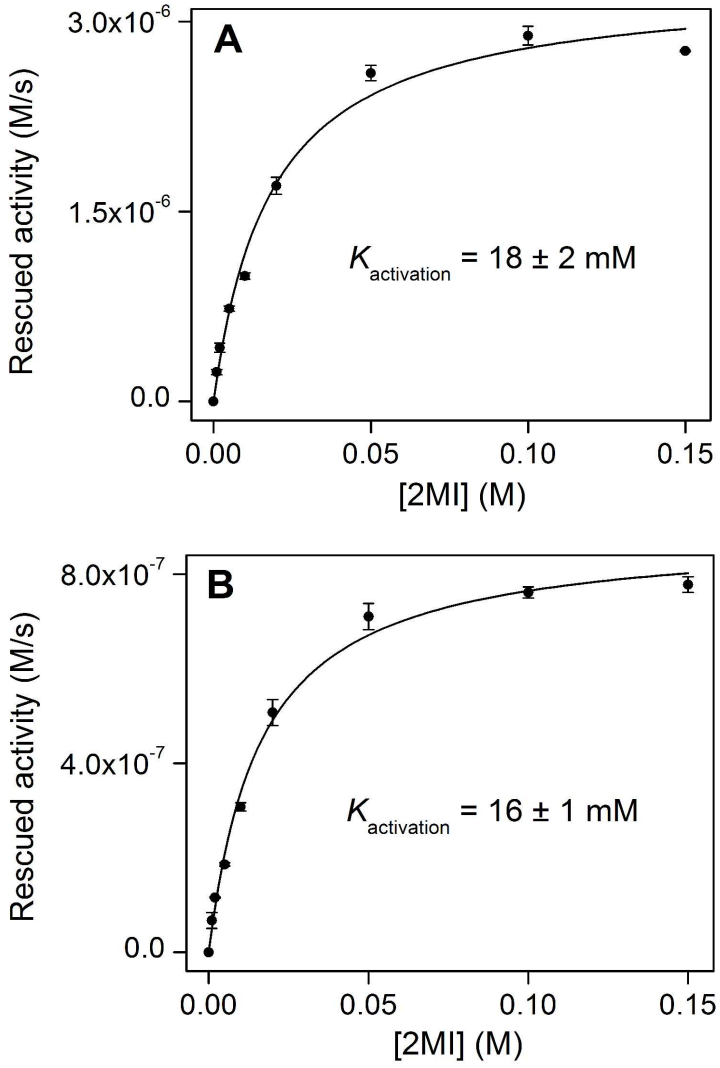

Figure S7. Comparison of enzymatic activities of cmTDO in the absence and presence of 2MI using 1-Me-L-Trp as the substrate. (A) WT-TDO, (B) Q73F, (C) H72S, (D) H72N. Formation of the product–*N*-formyl-methylkynurenine was monitored by the increase of absorbance at 321 nm. The kinetic traces were obtained in the presence of 1 mM 1-Me-L-Trp and 1 mM L-ascorbate with no exogenous 2MI (black), or 50 mM 2MI (red). The final concentration of enzyme in the reaction system was 0.45 μM for WT-TDO, 1 μM for Q73F, 3 μM for H72S and 5.5 μM for H72N. For each individual trace, the absorbance at the starting point was subtracted over the whole time course to correct for background.

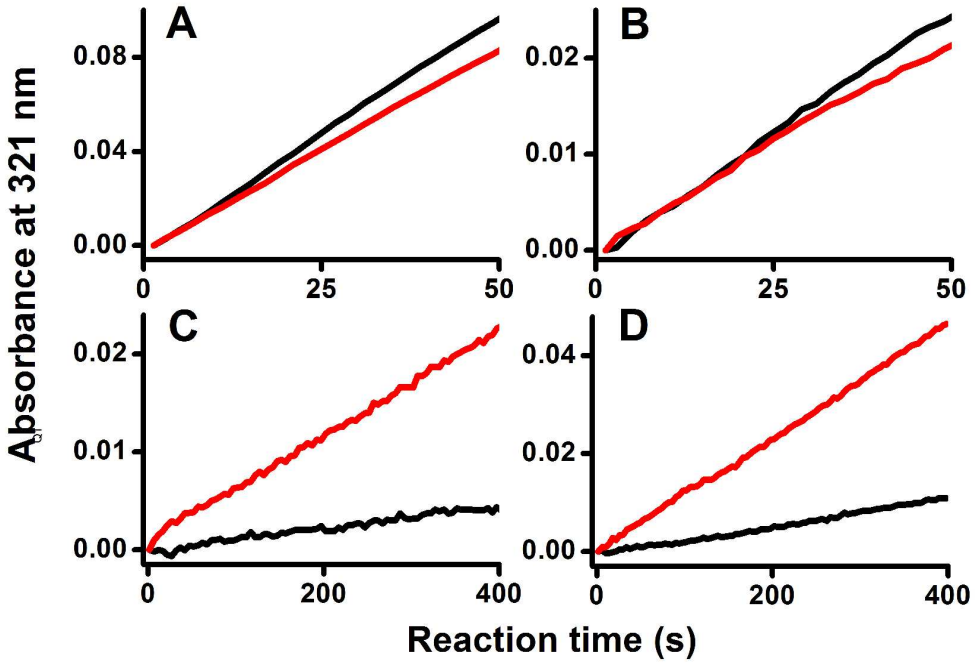

Figure S8. Time-resolved stopped-flow UV-Vis spectra of the reactions between cmTDO (15 μM) and H_2O_2 at 4 °C. (A) Q73F + 5 mM H_2O_2 (0 - 0.5 s); (B) H72S + 5 mM H_2O_2 (0 - 2.5 s); (C) H72S + 375 mM H_2O_2 (0 - 0.2 s); (D) H72S + 5 mM H_2O_2 with 50 mM 2MI in the reaction system (0 - 2.5 s). The insets are expanded views of the visible bands. The arrows indicate the trends of changes in the spectra.

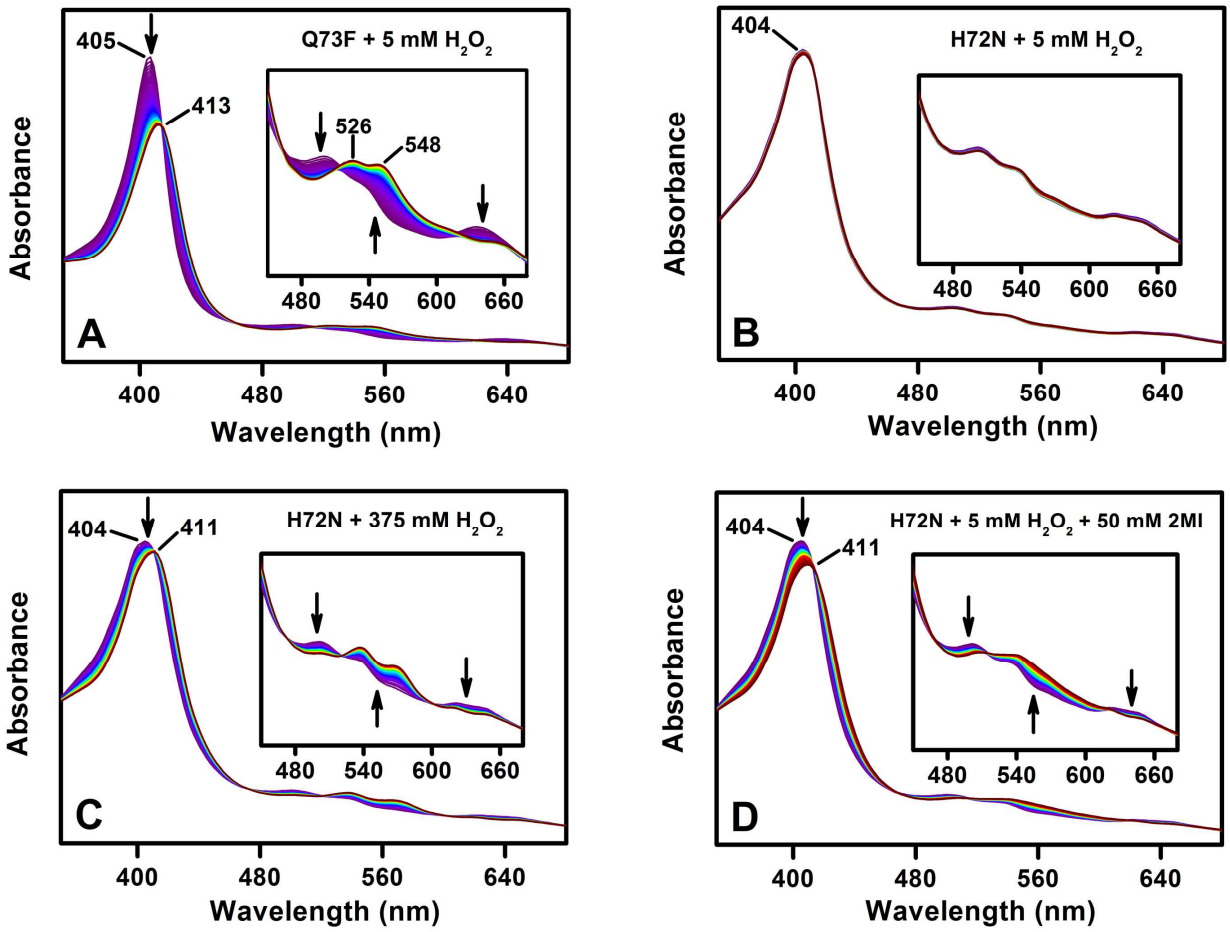

Figure S9. Time-resolved stopped-flow UV-Vis absorption difference spectra of the reactions between cmTDO (15 μM) and H_2O_2 at 4 °C. (A) Q73F + 5 mM H_2O_2 (0-0.5 s); (B) H72N + 375 mM H_2O_2 (0 - 0.2 s); (C) H72N + 5 mM H_2O_2 with 50 mM 2MI in the reaction system (0 - 2.5 s). The arrows indicate the trends of changes in the spectra. The "*" symbols indicate the three isosbestic points identified in the visible regions.